Published in final edited form as:
Traffic. 2008 November ; 9(11): 1915. doi:10.1111/j.1600-0854.2008.00805.x.

A PDZ-Binding Motif Controls Basolateral Targeting of Syndecan-1 Along the Biosynthetic Pathway in Polarized Epithelial Cells

Sandra Maday[1,2], **Eric Anderson**[1], **Henry C. Chang**[3], **James Shorter**[4], **Ayano Satoh**[1], **Jeff Sfakianos**[1,5], **Heike Fölsch**[6], **James M. Anderson**[7], **Zenta Walther**[8], and **Ira Mellman**[1,5,*]

[1] Department of Cell Biology, Ludwig Institute for Cancer Research, Yale University School of Medicine, New Haven, CT 06520, USA

[3] Department of Biological Sciences, Purdue University, West Lafayette, IN 47907, USA

[4] Department of Biochemistry and Biophysics, University of Pennsylvania School of Medicine, Philadelphia, PA 19104, USA

[5] Genentech, Inc., South San Francisco, CA 94080, USA

[6] Department of Biochemistry, Molecular Biology and Cell Biology, Northwestern University, Evanston, IL 60208, USA

[7] Department of Cell and Molecular Physiology, University of North Carolina, Chapel Hill, NC 27599, USA

[8] Department of Pathology, Yale University School of Medicine, New Haven, CT 06520, USA

Abstract

The cell surface proteoglycan, syndecan-1, is essential for normal epithelial morphology and function. Syndecan-1 is selectively localized to the basolateral domain of polarized epithelial cells and interacts with cytosolic PDZ (PSD-95, discs large, ZO-1) domain-containing proteins. Here, we show that the polarity of syndecan-1 is determined by its type II PDZ-binding motif. Mutations within the PDZ-binding motif lead to the mislocalization of syndecan-1 to the apical surface. In contrast to previous examples, however, PDZ-binding motif-dependent polarity is not determined by retention at the basolateral surface but rather by polarized sorting prior to syndecan-1's arrival at the plasma membrane. Although none of the four known PDZ-binding partners of syndecan-1 appears to control basolateral localization, our results show that the PDZ-binding motif of syndecan-1 is decoded along the biosynthetic pathway establishing a potential role for PDZ-mediated interactions in polarized sorting.

Keywords

basolateral; epithelia; PDZ; polarity; syndecan-1

The syndecans are a family of four type I transmembrane proteoglycans that are expressed in a developmentally regulated and tissue-specific manner (1,2). Syndecans function as coreceptors to modulate the activity of primary receptors at the cell surface, by binding a variety of growth factors and extracellular matrix components via covalently linked heparan sulfate

*Corresponding author: Ira Mellman, mellman.ira@gene.com.
[2]Current address: Department of Physiology, University of Pennsylvania School of Medicine, Philadelphia, PA 19104, USA

chains present in the ectodomain. Through these interactions, syndecans play diverse roles in cell–matrix and cell–cell adhesion, migration, and proliferation.

Syndecan-1 is expressed predominantly in epithelial cells, where it is uniquely restricted to the basolateral surface and maintains the epithelial phenotype (1,3–5). Downregulation of syndecan-1 causes epithelial cells to lose their cuboidal morphology, migrate and grow independent of anchorage (4). Yet, the mechanism by which syndecan-1 achieves basolateral distribution remains unknown.

As is true for many other basolateral membrane proteins, the cytoplasmic tail of syndecan-1 is essential for polarized targeting in Madin-Darby canine kidney (MDCK) cells (3). Deletion of the terminal 12 amino acids redistributes syndecan-1 from the basolateral membrane to the apical surface. Although this deletion removes a tyrosine residue that could potentially be part of a canonical basolateral targeting signal (6,7), a distinguishing feature of the syndecan-1 cytoplasmic domain is its highly conserved C-terminal type II PDZ (PSD-95, discs large, ZO-1)-binding motif, EFYA. Common to all four syndecans, the PDZ-binding motif binds to four PDZ domain-containing proteins: syntenin (which is localized to endosomes), synectin (which is localized to clathrin-coated structures and -uncoated vesicles), CASK (which is localized to the basolateral membrane) and synbindin (which is localized to the Golgi apparatus) (5,8–13). We wanted to determine whether interactions specified by this motif play an important role in establishing or maintaining polarity.

PDZ domains are modules of 80–90 amino acids that mediate protein–protein interactions by binding to motifs typically located at the C-terminus of transmembrane proteins (14). PDZ domains can interact with four types of degenerate PDZ-binding motifs: type I [X-(S/T)-X-Φ], type II (X-Φ-X-Φ), type III [X-(D/E)-X-Φ] and type IV [X-X-Ψ-(D/E)], where Φ and Ψ represent a hydrophobic and aromatic residue, respectively (15).

PDZ domain-containing proteins are associated with various aspects of polarity in epithelial cells. Formation of the tight junction is regulated by the evolutionarily conserved PDZ protein complex Par3/Par6/aPKC (16). PDZ proteins are also thought to facilitate selective retention at the apical or basolateral surface of plasma membrane proteins that contain PDZ-binding motifs (17,18). In such examples, proteins are delivered in a non-polarized fashion to both the apical and the basolateral surfaces, but then are stabilized or enriched at one or the other surface following plasma membrane insertion. The extent to which PDZ-mediated interactions might contribute to the polarized sorting of newly synthesized membrane proteins prior to arrival at the cell surface remains unclear. The fact that syndecan-1 interacts with PDZ domain proteins found in the Golgi and in endosomes suggests that such a mechanism is entirely possible.

Results and Discussion

The PDZ-binding motif of syndecan-1 is required for basolateral localization

To determine the localization of syndecan-1 in MDCK cells, stable cell lines were generated expressing wild-type (WT) syndecan-1. Cells were grown on filters to form a polarized monolayer, fixed, permeabilized, immunolabeled for syndecan-1 and analyzed by confocal microscopy. WT syndecan-1 was localized to the basolateral membrane of MDCK cells (Figure 1A). Monolayers were also labeled for gp58, the β subunit of the Na^+/K^+ ATPase, an endogenous basolateral marker (19).

Next, we asked if the PDZ-binding motif specifies basolateral localization of syndecan-1. We deleted the motif by truncation of the last two amino acids (ΔYA), a mutation that disrupts binding of syndecan-2 to syntenin (Figure 1B) (9). In contrast to WT, ΔYA syndecan-1 was

mislocalized largely to the apical membrane of MDCK cells (Figure 1C). These results suggest that the PDZ-binding motif is required for basolateral localization.

Initial attempts to quantify the distribution of syndecan-1 biochemically using available antibodies were unsuccessful. Hence, we developed an assay based on the expression of epitope-tagged syndecan-1. An myc epitope was introduced at the N-terminus, five residues after the predicted signal sequence (Figure 2A). Polarized MDCK cells were infected with recombinant adenoviruses encoding WT and ΔYA myc-syndecan-1 and its distribution at the cell surface was assessed 1 day post-infection. First, to determine that the myc-tagged construct behaved as did the WT protein, transfected cells were surface labeled for syndecan-1, processed for immunofluorescence (IF) and analyzed by confocal microscopy. WT myc-syndecan-1 was localized to the basolateral membrane and the ΔYA myc-syndecan-1 was mislocalized to the apical membrane, indicating that the myc epitope did not interfere with localization (Figure 2B).

To quantify the degree of mislocalization of ΔYA syndecan-1, polarized cells expressing either WT or ΔYA myc-syndecan-1 were surface biotinylated. Surface proteins in the apical or basolateral domain were selectively labeled with NHS-LC-LC-biotin, and domain-specific membrane proteins were retrieved with NeutrAvidin. Samples were digested with heparitinase I and chondroitin ABC lyase to remove glycosaminoglycan chains, enabling syndecan-1 to migrate as a discrete band by SDS–PAGE. Syndecan-1 levels in the apical or basolateral domain were determined by immunoblot analysis with an anti-myc antibody.

Consistent with the IF results, WT myc-syndecan-1 was detected predominantly (98%) at the basolateral membrane (Figure 2C). By contrast, ΔYA myc-syndecan-1 was found largely (73%) at the apical surface, although some (27%) remained at the basolateral domain (Figure 2C). These results confirm that the PDZ-binding motif of syndecan-1 is required for exclusive basolateral localization in polarized epithelial cells. To demonstrate that the polarity of the cells was not disrupted by adenoviral expression of syndecan-1, samples were also probed for gp114 (carcinoembryonic antigen-related cell adhesion molecule) (19). Gp114 was localized properly to the apical membrane, indicating that the observed mislocalization was specific to the truncated syndecan-1 (Figure 2C).

To further define the residues essential for basolateral localization, we introduced additional mutations within the PDZ-binding motif (EFYA). We removed the COOH-terminal alanine residue (ΔA), a mutation that disrupts binding of syndecan-2 to syntenin (9). We also generated a single point mutation of the tyrosine at position 33 to an alanine (Y33A). According to structural studies, the tyrosine at this position within the conserved PDZ-binding motif of syndecan-4 contacts the second PDZ domain of syntenin (20). The Y to A mutation also disrupts syndecan-2 and syntenin interactions, as measured by yeast two-hybrid assays (9). Finally we substituted the terminal A with a glutamate (A34E). Because the terminal residue of a PDZ-binding motif is typically hydrophobic, we hypothesized that the introduction of a charge at this site might disrupt binding to a PDZ domain (21).

To determine the effect of these mutations on syndecan-1 polarity, MDCK cells were infected with recombinant retroviruses encoding WT, ΔYA, ΔA, Y33A and A34E myc-syndecan-1, and stable cell lines were generated. Polarized monolayers were stained for the surface appearance of syndecan-1 and gp58, processed for IF and analyzed by confocal microscopy. Consistent with our previous observations (Figures 1A,C, and 2B,C), retrovirally expressed WT syndecan-1 was localized to the basolateral membrane, whereas ΔYA syndecan-1 was mislocalized to the apical surface (Figure 3A). Similar to ΔYA syndecan-1, ΔA syndecan-1 was largely mislocalized to the apical domain. In contrast, Y33A syndecan-1 was distributed predominantly at the basolateral surface; however, occasionally we observed cells with apical

mislocalization. Finally, A34E syndecan-1 was localized to the basolateral surface, similar to WT syndecan-1. In each of the stable cell lines, gp58 was basolateral, indicating that the overall polarity of the cells was not disrupted.

To quantify the degree of mislocalization of each syndecan-1 mutant, cell lines were surface biotinylated as described above. Consistent with the IF, WT syndecan-1 was basolateral (94%) (Figure 3B,C). ΔYA and ΔA syndecan-1 were mislocalized to the apical surface by 55 and 48%, respectively. Y33A syndecan-1 was distributed 82% on the basolateral surface, with a slight increase in apical mis-sorting (18% with Y33A as compared with 6% with WT). A34E syndecan-1 was localized 94% to the basolateral membrane, comparable with WT syndecan-1. To demonstrate that the overall polarity of the cells was not disrupted by retroviral expression of syndecan-1, samples were also probed for the endogenous apical marker, gp135 (canine orthologue of podocalyxin) (34).

Taken together, these data show that the PDZ-binding motif in the cytoplasmic tail of syndecan-1 is essential for basolateral localization. Truncation of the terminal two amino acids (ΔYA), or just the terminal alanine, of this motif mislocalized the receptor to the apical surface. These results support an essential role for a functional PDZ-binding motif in determining the basolateral polarity of syndecan-1, as found for other basolateral, as well as apical, membrane proteins that contain PDZ-binding motifs (22–24). The lack of mislocalization of Y33A syndecan-1 was surprising, although a functional requirement for this tyrosine residue in other PDZ interactions has not been shown, despite the prediction of its importance from structural studies. We also did not observe a defect in the basolateral distribution of A34E syndecan-1. It is possible that a charged residue at the terminal position may be tolerated by the PDZ interaction(s) involving syndecan-1, as is the case in a newly emerging class of PDZ domains (25).

Knockdown of syntenin, synectin, CASK or synbindin does not mislocalize syndecan-1 to the apical membrane

We sought to identify the PDZ protein(s) that mediate syndecan-1 polarity. The PDZ-binding motif in the syndecan tails interacts with the PDZ proteins syntenin, synectin, CASK and synbindin (5,9–11). Using RNAi, we examined how syntenin, synectin, CASK and synbindin contribute to syndecan-1 polarity.

To deplete each target protein, short hairpin RNAs were designed against relevant canine sequences. We used recombinant retroviruses to express shRNAs in MDCK cells and generate stable cell lines. The degree of knockdown was determined by quantitative immunoblotting of whole cell lysates. We reduced syntenin, synectin and CASK expression in MDCK cells by 91, 88 and 75%, respectively (Table 1 and Figure S1A). Three different shRNAs were designed to target synbindin; however, the degree of knockdown could not be determined with the available antibodies.

To determine the effects of PDZ protein depletion on syndecan-1 localization, polarized monolayers of retroviral cell lines were infected with an adenovirus encoding WT myc-syndecan-1 and its distribution at the cell surface was assessed. Syndecan-1 was localized to the basolateral membrane in empty virus control cells, indicating that polarity was not disrupted by retroviral infection (Figure S1B). Syndecan-1 was also localized to the basolateral membrane in all the knockdown cells, indicating that reduced levels of syntenin, synectin, CASK and potentially synbindin did not affect syndecan-1 localization (Table 1 and Figure S1B).

Depletion of a single PDZ protein may be insufficient to mislocalize syndecan-1 to the apical membrane because of redundant and/or compensatory mechanisms. Therefore, we next

depleted syntenin, synectin and CASK, in combinations of two. Cells stably expressing an shRNA to knockdown syntenin or synectin were infected with retroviruses encoding an shRNA targeting CASK or synectin.

In cells where syntenin expression was reduced by 87%, synectin was also depleted by 79% (Table 1 and Figure S2A). In cells where syntenin expression was reduced by 78%, CASK expression was then reduced by 77%. Finally, in cells stably expressing an shRNA to reduce synectin expression by 83%, the expression level of CASK was reduced by 71%.

In the syntenin or synectin single-knockdown cells infected with an empty virus control, syndecan-1 was distributed on the basolateral membrane (Figure S2B). In double-knockdown cells, syndecan-1 was also localized to the basolateral membrane, indicating that even pairwise reduction of syntenin and synectin, or syntenin and CASK, or CASK and synectin did not affect syndecan-1 localization (Table 1 and Figure S2B). Thus, either the degree of knockdown was insufficient to eliminate function, or an as yet unidentified PDZ protein or adaptor mediates the basolateral distribution of syndecan-1. Perhaps, a non-PDZ protein recognizes residues within the PDZ-binding motif. Knockdown of AP1B or AP4 subunits had no effect on syndecan-1 polarity (not shown).

Syndecan-1 is sorted directly to the basolateral membrane

Irrespective of the identity of the relevant adaptor for syndecan-1, it was critical to determine the mechanism of basolateral polarity. Syndecan-1 may be selectively retained at the basolateral membrane following random delivery to both apical and basolateral surfaces, as suggested for other PDZ-binding motif-dependent membrane proteins such as CFTR (18). Alternatively, syndecan-1 may be sorted in an intracellular compartment, such as the *trans* Golgi network (TGN) or recycling endosomes, and targeted directly to the basolateral membrane. Finally, syndecan-1 may be delivered initially to the apical domain, and then be transcytosed to the basolateral membrane.

To distinguish among these possibilities, a pulse–chase experiment combined with cell surface biotinylation was performed on polarized MDCK cells expressing WT or ΔYA myc-syndecan-1. Newly synthesized proteins were metabolically labeled with ^{35}S-methionine and ^{35}S-cysteine for 15 min at 37° C, and then chased for various times in non-radiolabeled medium. Apical or basolateral appearance was detected by domain-specific surface biotinylation. Total syndecan-1 protein was immunoprecipitated and biotinylated domain-specific surface protein was retrieved with NeutrAvidin. Samples were then digested with heparitinase I and chondroitinase ABC lyase. To quantify syndecan-1 levels in the apical or basolateral domain, radioactivity was determined using a phosphorimager.

WT syndecan-1 first appeared on only the basolateral membrane at 30 min; this vectorial basolateral insertion was maintained for at least 3 h of chase (Figure 4A,B). Failure to detect syndecan-1 on the apical membrane is inconsistent with the models of selective retention and transcytosis. These results suggest that syndecan-1 is sorted intracellularly and targeted directly to the basolateral membrane.

In contrast to WT, ΔYA syndecan-1 first appeared on both apical and basolateral domains at approximately 30 and 60 min (Figure 4A,B). Quantification showed that this non-polarized distribution was maintained on average until approximately 120 min, at which time ΔYA syndecan-1 appeared to accumulate more selectively on the apical membrane (Figure 4B). It is unclear whether this final distribution is achieved by selective retention at the apical domain, or rather transcytosis from the basolateral surface. These results indicate that truncation of the PDZ-binding motif disrupts selective insertion into the basolateral membrane, leading to randomized insertion into both apical and basolateral domains. Hence, the PDZ-binding motif

contributes to the polarized sorting of newly synthesized syndecan-1 prior to arrival at the basolateral surface.

We have demonstrated that the PDZ-binding motif regulates the intracellular sorting of newly synthesized syndecan-1 and targets it directly to the basolateral surface. This result is distinct from previous reports in polarized epithelial cells, which implicate PDZ-binding motifs only after surface arrival. For example, the PDZ-binding motif of BGT-1 selectively stabilizes the transporter at the basolateral surface; truncation of the PDZ-binding motif results in internalization (17). The PDZ-binding motif of CFTR retains the channel at the apical domain following random delivery to both apical and basolateral surfaces (18). Without the PDZ-binding motif, internalized CFTR is unable to recycle back to the apical surface from endocytic compartments.

Our findings suggest that the PDZ-binding motif of syndecan-1 is decoded along the biosynthetic pathway, prior to appearance at the plasma membrane. Accordingly, our data predict a potential role for PDZ proteins in polarized sorting in the TGN and/or recycling endosomes. Similar PDZ-binding motif-mediated interactions function early in the secretory pathway of non-polarized cells and regulate pro-TGF-α transport to the cell surface (26). Another potential example is Kir 2.3, a K^+ channel whose direct insertion into the basolateral membrane depends on its cytoplasmic tail, which harbors a PDZ-binding motif (27). While the PDZ-binding motif is important for cell surface expression, a role in vectorial transport has not been established (27,28). Several PDZ proteins, e.g. CAL and LIN-10, localize to the TGN in polarized epithelial cells, with LIN-10 having an essential if unspecified role in controlling basolateral localization of EGF receptors (LET-23) in *Caenorhabditis elegans* (22,29,30). Other PDZ proteins, e.g. syntenin, appear to localize to endosomes (8). Although it was not possible to identify the relevant intracellular adaptor for syndecan-1, our findings provide an important conceptual context to explore the functional significance of PDZ proteins associated with intracellular compartments.

Materials and Methods

Antibodies

The rat anti-mouse syndecan-1 (clone 281-2) monoclonal antibody was provided by A. Rapraeger (University of Wisconsin-Madison), and also purchased from BD Pharmingen. The hybridoma expressing mouse anti-gp135 IgGs was provided by K. Simons (Max-Planck-Institute of Molecular Cell Biology and Genetics, Dresden, Germany). The 6.23.3 and Y652 hybridomas expressing mouse anti-gp58 and anti-gp114 IgGs, respectively, were obtained from the American Type Culture Collection. Rabbit polyclonal antibodies were raised against the N-terminal domain of MDCK syntenin (amino acids 2–109) fused to the C-terminus of glutathione S-transferase. The rabbit anti-c-Myc (clone A-14) and goat anti-synectin (clone N-19) polyclonal antibodies were purchased from Santa Cruz Biotechnologies. The mouse anti-CASK monoclonal antibody (clone 7) was obtained from BD Transduction. Alexa-labeled secondary antibodies were purchased from Invitrogen. Horseradish peroxidase-conjugated secondary antibodies were purchased from Pierce and Sigma.

Cell lines

MDCK II cells were cultured in MEM (Invitrogen) supplemented with 10% FBS, 2 mM L-glutamine, 100 U/mL penicillin and 100 μg/mL streptomycin. GP2-293 cells for retrovirus production were maintained in DMEM supplemented with 10% FBS, 2 mM L-glutamine, 100 U/mL penicillin and 100 μg/mL streptomycin. All cell lines were maintained at 37°C in a 5% CO_2 incubator.

Cloning and expression of syndecan-1

Constructs were generated by polymerase chain reaction (PCR) using mouse syndecan-1 complementary DNA (cDNA) as a template (Genbank accession no. X15487). To generate the ΔYA truncation mutant, a stop codon was placed after the C-terminal phenylalanine at amino acid position 309. To generate the ΔA truncation mutant, a stop codon was placed after the tyrosine at position 310. The Y33A point mutation was generated by mutating the codon of tyrosine 310 from 'TAC' to 'GCC'. The A34E point mutation was generated by mutating the codon of alanine 311 from 'GCC' to 'GAG'. Using nested PCR, an myc epitope (EQKLISEEDL) was introduced at the N-terminus after amino acid 22, five residues after the putative 17 amino acid signal sequence. All constructs were verified by sequencing analysis.

To generate stable cell lines (Figure 1), WT and ΔYA syndecan-1 PCR products were subcloned into pBGS as *Eco*RI/*Xba*I fragments. MDCK II cells were transfected with WT and ΔYA syndecan-1 constructs, and selected in MEM supplemented with 10% FBS, 2 mM L-glutamine, 100 U/mL penicillin, 100 μg/mL streptomycin and 0.9 mg/mL G418. Individual clones were selected and amplified.

To generate recombinant adenoviruses, WT and ΔYA myc-syndecan-1 PCR products were subcloned into pShuttle-CMV (AdEasy Vector System; Q-BIO gene) as *Kpn*I/*Xba*I fragments and then recombined into pAdeasy-1. Recombinant adenoviruses were generated using the AdEasy Vector System (Q-BIO gene).

To generate myc-syndecan-1 stable cell lines (Figure 3), WT, ΔYA, ΔA, Y33A and A34E myc-syndecan-1 PCR products were subcloned into pQCXIP (BD Biosciences) as *Bam*HI/*Eco*RI fragments. GP2-293 cells were cotransfected with the pQCXIP vector, along with a vector expressing VSV-G protein (31), and incubated at 37°C in a 5% CO_2 incubator. Medium containing recombinant retrovirus was collected and passed through a 0.45-μm filter unit. MDCK cells were spin infected with recombinant retrovirus, supplemented with 6 mg/mL polybrene (American Bioanalytical), at 582 × ***g*** for 1 h at 4°C. Twenty-four hours post-infection, stable lines were selected with MEM supplemented with 0.5 μg/mL puromycin (Sigma).

Immunofluorescence

MDCK cells were plated onto 12-mm transwell filter supports (0.4-μm pore size; Corning, Inc. Life Sciences) at a density of 4×10^5 cells per well and cultured for 4 days. On the fourth day, cells were analyzed by IF, unless the assay required adenoviral expression of syndecan-1. In that case, on the fourth day, cells were infected with adenovirus for 1 h at 37°C. Twenty hours post-infection, cells were analyzed by IF. For surface labeling, filters were excised from the filter support, washed twice in ice-cold PBS^{++} (2.7 mM KCl, 1.5 mM KH_2PO_4, 137 mM NaCl, 8.1 mM Na_2HPO_4, 1 mM $CaCl_2$ and 0.5 mM $MgCl_2$) and incubated in primary antibody (if necessary, the antibody was diluted in PBS^{++}) for 15 min on ice. The cells were then washed twice in ice-cold PBS^{++} and fixed in 3% paraformaldehyde (PFA)/PBS^{++} for 15 min at room temperature. The cells were washed twice in PBS^{++} and blocked and permeabilized in 2% (w/v) BSA, 0.1% (w/v) saponin (Sigma), and PBS^{++} (blocking buffer) for 1 h at room temperature. The cells were incubated in secondary antibody, diluted in blocking buffer, for 1 h, and then washed 5 times for 6 min each in blocking buffer. The filters were then mounted in DABCO [10% (w/v) DABCO (Sigma), 50% (w/v) glycerol and PBS^{++}].

For total labeling, cells were washed in PBS^{++} and fixed in 3% PFA in PBS^{++} for 15 min at room temperature. The cells were washed again in PBS^{++}, and blocked and permeabilized in 2% BSA, 0.1% saponin, and PBS^{++} for 1 h at room temperature. The cells were then incubated in primary antibody (diluted in blocking buffer) for 1 h at room temperature, washed 5 times

for 6 min each in blocking buffer, incubated in secondary antibody (diluted in blocking buffer) for 1 h, washed 5 times for 6 min each, and then mounted in DABCO.

Samples were analyzed using an LSM 510 confocal microscope (Carl Zeiss MicroImaging, Inc.) with a × 40 water immersion objective, and images were obtained with LSM software (Carl Zeiss MicroImaging, Inc.).

Cell surface biotinylation

MDCK cells were plated onto 24-mm transwell filter supports (0.4-μm pore size) at a density of 1.6×10^6 cells per well and cultured for 4 days. On the fourth day, cells were analyzed by surface biotinylation, unless the assay required adenoviral expression of syndecan-1. In that case, on the fourth day, cells were infected with adenovirus for 1 h at 37°C. Twenty hours post-infection, cells were analyzed by surface biotinylation. Cells were placed on ice and washed 3 times for 5 min each in ice-cold PBS^{++}. Either the apical or basolateral domain was then biotinylated using a solution of 1.5 mg/mL EZ-Link-Sulfo-NHS-LC-LC-Biotin (Pierce) diluted in PBS^{++}. The biotinylation reaction proceeded for 20 min on ice. The biotinylation reagent was then removed, and replaced with fresh biotinylation reagent, and incubated for another 20 min. The filters were then washed 3 times for 5 min each in 100 mM glycine in PBS^{++}, followed by 2 washes for 5 min each in 20 mM glycine in PBS^{++}. The filters were then cut out of the filter support and the cells were harvested in 1.25 mL lysis buffer [1% Triton-X-100, 0.1% SDS, 20 mM glycine, 1× complete protease inhibitor cocktail tablet with ethylenediaminetetraacetic acid (EDTA) (Roche Diagnostics) and PBS^{CMF}]. Cells were scraped in lysis buffer, passaged four times through a 22G needle, transferred to eppendorf tubes and incubated 30 min on ice. The samples were then spun 16 000 × ***g*** for 15 min at 4°C. Nine hundred microliters of the supernatant (about 0.36 μg/μL of total protein) was transferred to 20-μL bed volume of NeutrAvidin beads (Pierce) that had been previously blocked in total cell lysates of MDCK cells, not expressing mouse syndecan-1, prepared in the same manner as just described for the biotinylated samples. The beads were rotated end over end for 16 h at 4°C and were washed 3 times in lysis buffer, twice in high-salt buffer (0.1% Triton-X-100, 350 mM NaCl and PBS^{CMF}), once in PBS^{CMF} and 3 times in heparitinase buffer (150 mM NaCl, 5 mM $CaCl_2$, 50 mM NaOAc and 50 mM HEPES, pH 6.5). The samples were then resuspended in 50 μL of heparitinase buffer and 1.0 μL of heparitinase I (Seikagaku America) and chondroitin ABC lyase (ICN Biomedical, Inc.) was added to obtain a final concentration of 2.4×10^{-3} and 0.1 U/mL, respectively. Samples were incubated for 2 h at 37°C in an air incubator. After the 2-h incubation, 1.0 μL of each enzyme was added fresh and the samples were incubated for another 2 h. SDS–PAGE [5×, 10% SDS (w/v), 50% glycerol (w/v), 20% (v/v) β-mercaptoethanol, 0.05% (w/v) bromophenol blue and 300 mM Tris, pH 6.8] sample buffer was added and the samples were loaded onto an SDS–PAGE gel. Protein was transferred onto Immobilon P PVDF membrane (Millipore Corporation) using the wet transfer tank apparatus (BIO-RAD). The membrane was washed in PBS^{CMF} and then fixed in 0.25% glutaraldehyde in PBS^{CMF} for 30 min at room temperature. The membrane was rinsed in water, Tris-buffered saline (TBS) and then analyzed by western blotting. In Figure 2C, two 10% gels were run for each of the WT and ΔYA samples. One gel was analyzed for the myc epitope, while the second gel was analyzed for gp114. In Figure 3B, an 8% gel was analyzed by immunoblot for the myc epitope and re-probed for gp135.

shRNA/RNA interference

The full-length nucleotide sequence of MDCK syntenin and a partial sequence of MDCK synectin were cloned from an MDCK cDNA library and verified by sequencing analysis. The full-length nucleotide sequences of canine synectin, CASK and synbindin were obtained from Genbank; Genbank accession numbers XM_542018, BU750917 and XM_536548, respectively.

Oligonucleotides encoding an shRNA were designed following the pSUPER RNAi system (Oligoengine), annealed and cloned into the pSUPER vector at the *Bgl*II/*Hin*dIII sites (32). The 19-nucleotide target sequence for each PDZ protein was as follows: GGATAGTACCGGACATGTT (MDCK Syntenin), TAGAGGTGTTCAAGTCAGA (Canine Synectin for single RNAi), GGTAGATGACCTGCTGGAG (MDCK Synectin for double RNAi), TGGCATCAGTGTGGCTAAC (Canine CASK RNAi), GCTTATGCTGGCCTCTATG (Canine Synbindin RNAi #1), TTGGTTCCCAGCTGTCTCC (Canine Synbindin RNAi #2) and GAATCCATTCTACTCCCTG (Canine Synbindin RNAi #3). An *Eco*RI/*Xho*I fragment, consisting of the H1 promoter and the shRNA, was then transferred from pSUPER into the retroviral vectors, RVH1-puromycin or RVH1-hygromycin (31,33). All constructs were verified by sequencing analysis. GP2-293 cells were cotransfected with the RVH1 vector, along with a vector expressing VSV-G protein (31), and incubated at 37°C in a 5% CO_2 incubator. Medium containing recombinant retrovirus was collected, passed through an 0.45-μm filter unit and spin concentrated at 50 000 × ***g*** for 2 h at 4°C. MDCK cells were spin infected with recombinant retrovirus, supplemented with 6 mg/mL polybrene (American Bioanalytical), at 582 × ***g*** for 1 h at 4°C. Twenty-four hours post-infection, stable lines were selected with MEM supplemented with 4.0 μg/mL puromycin (Sigma) or 800 μg/mL hygromycin (Invitrogen).

For quantitative western blotting, confluent monolayers were washed 3 times in PBS^{++}, scraped in lysis buffer (1% Triton-X-100, 0.5% deoxycholate, 0.1% SDS, 150 mM NaCl, 1× complete protease inhibitor cocktail tablet with EDTA and 50 mM Tris-HCl, pH 7.4), passaged four times through a 22-guage needle, transferred to an eppendorf tube and incubated on ice for 30 min. The samples were then spun 16 000 × ***g*** for 15 min at 4°C, and the supernatant was transferred to a new eppendorf tube. A BCA protein assay (Pierce) was performed to determine the protein concentration of each sample. Equal amounts of total protein for the empty virus control and knockdown samples were loaded onto an SDS–PAGE gel. The degree of knockdown was then quantified by loading serial dilutions of the empty virus control lysates. The maximum amount of protein loaded onto the gel was adjusted accordingly for each antibody used for western blotting, to ensure that the serial dilutions (and specific protein in knockdown cell lines) were within the linear range. Protein was transferred onto Immobilon P PVDF (Millipore) using a semidry transfer apparatus (BIO-RAD), and analyzed by western blotting.

Pulse-chase cell surface biotinylation

MDCK cells were plated onto 24-mm transwell filters at a density of 8×10^5 cells per well, and cultured for 4 days with daily changes of medium. Cells were infected with adenovirus for 1 h at 37°C. Twenty hours after infection, the cells were washed in warm PBS^{++} and starved for 30 min at 37°C in a 5% CO_2 incubator in MEM-met-cys (ICN) supplemented with 10% dialyzed FBS (Invitrogen) and 2 mM L-glutamine. Proteins were pulse labeled for 15 min at 37°C with 2 mCi/mL [^{35}S]Met/Cys (EXPRE^{35}S^{35}S Protein Labeling mix, NEN Life Science Products, Inc.) in MEM-met-cys supplemented with 10% dialyzed FBS and 2 mM L-glutamine. The cells were then washed in warm PBS^{++} and chased for 0, 30, 60, 120 and 180 min in MEM supplemented with 10% FBS and 5× methionine and cysteine. Following each time point, the cells were placed on ice, biotinylated and total cell lysates were prepared as described in the biotinylation section. Nine hundred microliters of supernatant was transferred to 20-μL bed volume of protein A beads (Zymed) that were conjugated to an anti-myc antibody (4 μg Ab/sample). The beads were rotated end over end for 16 h at 4°C, washed 3 times in lysis buffer and resuspended in 100 μL SDS buffer (2% SDS, 100 mM NaCl, 20 mM glycine and 20 mM Tris–HCl, pH 8.0). The samples were incubated at 100°C for 2 min, cooled on ice for 30 seconds and vortexed for 30 seconds. One milliliter of lysis buffer was added to the beads and the samples were vortexed for 30 seconds. Nine hundred microliters was transferred to 20-

μL bed volume of NeutrAvidin beads that had been previously blocked in total cell lysate of uninfected WT MDCK cells prepared in the same manner as described for biotinylated samples. The NeutrAvidin beads were incubated end over end for 1 h at 4°C and were washed 3 times in lysis buffer, once in 0.2% SDS in PBS^{CMF}, once in PBS^{CMF}, twice in high-salt buffer (0.1% Triton-X-100, 350 mM NaCl and PBS^{CMF}), once in PBS^{CMF} and 3 times in heparitinase buffer. Beads were resuspended in 50 μL heparitinase buffer and digested as described in the biotinylation section. SDS–PAGE (5×) sample buffer was added and sample was loaded onto a 10% SDS–PAGE gel. The gel was stained with Coomassie brilliant blue R250 (2 g/L), dried onto Whatman paper and exposed to a phosphorimager cassette. Radioactivity was detected using a phosphorimager (model Storm 860; GE Healthcare). The intensity of each band was quantified using Adobe Photoshop. Membrane distribution was plotted as a percentage of total apical and basolateral signal for each time point. Mean values from two independent experiments were graphed using Excel (Microsoft Office), and error bars indicate standard deviation.

Supplementary Material

Refer to Web version on PubMed Central for supplementary material.

Acknowledgments

We thank A. Rapraeger for anti-syndecan-1 antibody, B. Burbach for technical advice, C. Chalouni for help with confocal microscopy and Mark Velleca for the MDCK cDNA library. Supported by the Ludwig Institute for Cancer Research and the NIH (RO1GM29765 and PO1CA46128 to I. M. and K08DK059341 to Z.W.).

References

1. Kim CW, Goldberger OA, Gallo RL, Bernfield M. Members of the syndecan family of heparan sulfate proteoglycans are expressed in distinct cell-, tissue-, and development-specific patterns. Mol Biol Cell 1994;5:797–805. [PubMed: 7812048]
2. Bernfield M, Gotte M, Park PW, Reizes O, Fitzgerald ML, Lincecum J, Zako M. Functions of cell surface heparan sulfate proteoglycans. Annu Rev Biochem 1999;68:729–777. [PubMed: 10872465]
3. Miettinen HM, Edwards SN, Jalkanen M. Analysis of transport and targeting of syndecan-1: effect of cytoplasmic tail deletions. Mol Biol Cell 1994;5:1325–1339. [PubMed: 7696713]
4. Kato M, Saunders S, Nguyen H, Bernfield M. Loss of cell surface syndecan-1 causes epithelia to transform into anchorage-independent mesenchyme-like cells. Mol Biol Cell 1995;6:559–576. [PubMed: 7545031]
5. Cohen AR, Woods DF, Marfatia SM, Walther Z, Chishti AH, Anderson JM. Human CASK/LIN-2 binds syndecan-2 and protein 4.1 and localizes to the basolateral membrane of epithelial cells. J Cell Biol 1998;142:129–138. [PubMed: 9660868]
6. Matter K, Mellman I. Mechanisms of cell polarity: sorting and transport in epithelial cells. Curr Opin Cell Biol 1994;6:545–554. [PubMed: 7986532]
7. Rodriguez-Boulan E, Kreitzer G, Musch A. Organization of vesicular trafficking in epithelia. Nat Rev Mol Cell Biol 2005;6:233–247. [PubMed: 15738988]
8. Fialka I, Steinlein P, Ahorn H, Bock G, Burbelo PD, Haberfellner M, Lottspeich F, Paiha K, Pasquali C, Huber LA. Identification of syntenin as a protein of the apical early endocytic compartment in Madin-Darby canine kidney cells. J Biol Chem 1999;274:26233–26239. [PubMed: 10473577]
9. Grootjans JJ, Zimmermann P, Reekmans G, Smets A, Degeest G, Durr J, David G. Syntenin, a PDZ protein that binds syndecan cytoplasmic domains. Proc Natl Acad Sci U S A 1997;94:13683–13688. [PubMed: 9391086]
10. Ethell IM, Hagihara K, Miura Y, Irie F, Yamaguchi Y. Synbindin, A novel syndecan-2-binding protein in neuronal dendritic spines. J Cell Biol 2000;151:53–68. [PubMed: 11018053]
11. Gao Y, Li M, Chen W, Simons M. Synectin, syndecan-4 cytoplasmic domain binding PDZ protein, inhibits cell migration. J Cell Physiol 2000;184:373–379. [PubMed: 10911369]

12. Lou X, McQuistan T, Orlando RA, Farquhar MG. GAIP, GIPC and Gαi3 are concentrated in endocytic compartments of proximal tubule cells: putative role in regulating megalin's function. J Am Soc Nephrol 2002;13:918–927. [PubMed: 11912251]
13. Naccache SN, Hasson T, Horowitz A. Binding of internalized receptors to the PDZ domain of GIPC/synectin recruits myosin VI to endocytic vesicles. Proc Natl Acad Sci U S A 2006;103:12735–12740. [PubMed: 16908842]
14. Jelen F, Oleksy A, Smietana K, Otlewski J. PDZ domains – common players in the cell signaling. Acta Biochim Pol 2003;50:985–1017. [PubMed: 14739991]
15. Vaccaro P, Dente L. PDZ domains: troubles in classification. FEBS Lett 2002;512:345–349. [PubMed: 11852108]
16. Joberty G, Petersen C, Gao L, Macara IG. The cell-polarity protein Par6 links Par3 and atypical protein kinase C to Cdc42. Nat Cell Biol 2000;2:531–539. [PubMed: 10934474]
17. Perego C, Vanoni C, Villa A, Longhi R, Kaech SM, Frohli E, Hajnal A, Kim SK, Pietrini G. PDZ-mediated interactions retain the epithelial GABA transporter on the basolateral surface of polarized epithelial cells. EMBO J 1999;18:2384–2393. [PubMed: 10228153]
18. Swiatecka-Urban A, Duhaime M, Coutermarsh B, Karlson KH, Collawn J, Milewski M, Cutting GR, Guggino WB, Langford G, Stanton BA. PDZ domain interaction controls the endocytic recycling of the cystic fibrosis transmembrane conductance regulator. J Biol Chem 2002;277:40099–40105. [PubMed: 12167629]
19. Fullekrug J, Shevchenko A, Shevchenko A, Simons K. Identification of glycosylated marker proteins of epithelial polarity in MDCK cells by homology driven proteomics. BMC Biochem 2006;7:8. [PubMed: 16533391]
20. Kang BS, Cooper DR, Devedjiev Y, Derewenda U, Derewenda ZS. Molecular roots of degenerate specificity in syntenin's PDZ2 domain: reassessment of the PDZ recognition paradigm. Structure 2003;11:845–853. [PubMed: 12842047]
21. Kim E, Niethammer M, Rothschild A, Jan YN, Sheng M. Clustering of Shaker-type K^+ channels by interaction with a family of membrane-associated guanylate kinases. Nature 1995;378:85–88. [PubMed: 7477295]
22. Kaech SM, Whitfield CW, Kim SK. The LIN-2/LIN-7/LIN-10 complex mediates basolateral membrane localization of the *C. elegans* EGF receptor LET-23 in vulval epithelial cells. Cell 1998;94:761–771. [PubMed: 9753323]
23. Muth TR, Ahn J, Caplan MJ. Identification of sorting determinants in the C-terminal cytoplasmic tails of the γ-aminobutyric acid transporters GAT-2 and GAT-3. J Biol Chem 1998;273:25616–25627. [PubMed: 9748227]
24. Moyer BD, Denton J, Karlson KH, Reynolds D, Wang S, Mickle JE, Milewski M, Cutting GR, Guggino WB, Li M, Stanton BA. A PDZ-interacting domain in CFTR is an apical membrane polarization signal. J Clin Invest 1999;104:1353–1361. [PubMed: 10562297]
25. Vaccaro P, Brannetti B, Montecchi-Palazzi L, Philipp S, Helmer Citterich M, Cesareni G, Dente L. Distinct binding specificity of the multiple PDZ domains of INADL, a human protein with homology to INAD from *Drosophila melanogaster*. J Biol Chem 2001;276:42122–42130. [PubMed: 11509564]
26. Fernandez-Larrea J, Merlos-Suarez A, Urena JM, Baselga J, Arribas J. A role for a PDZ protein in the early secretory pathway for the targeting of proTGF-α to the cell surface. Mol Cell 1999;3:423–433. [PubMed: 10230395]
27. Le Maout S, Welling PA, Brejon M, Olsen O, Merot J. Basolateral membrane expression of a K^+ channel, Kir 2.3, is directed by a cytoplasmic COOH-terminal domain. Proc Natl Acad Sci U S A 2001;98:10475–10480. [PubMed: 11504929]
28. Olsen O, Liu H, Wade JB, Merot J, Welling PA. Basolateral membrane expression of the Kir 2.3 channel is coordinated by PDZ interaction with Lin-7/CASK complex. Am J Physiol Cell Physiol 2002;282:C183–C195. [PubMed: 11742811]
29. Whitfield CW, Benard C, Barnes T, Hekimi S, Kim SK. Basolateral localization of the *Caenorhabditis elegans* epidermal growth factor receptor in epithelial cells by the PDZ protein LIN-10. Mol Biol Cell 1999;10:2087–2100. [PubMed: 10359617]

30. Cheng J, Moyer BD, Milewski M, Loffing J, Ikeda M, Mickle JE, Cutting GR, Li M, Stanton BA, Guggino WB. A Golgi-associated PDZ domain protein modulates cystic fibrosis transmembrane regulator plasma membrane expression. J Biol Chem 2002;277:3520–3529. [PubMed: 11707463]

31. Schuck S, Manninen A, Honsho M, Fullekrug J, Simons K. Generation of single and double knockdowns in polarized epithelial cells by retrovirus-mediated RNA interference. Proc Natl Acad Sci U S A 2004;101:4912–4917. [PubMed: 15051873]

32. Brummelkamp TR, Bernards R, Agami R. A system for stable expression of short interfering RNAs in mammalian cells. Science 2002;296:550–553. [PubMed: 11910072]

33. Barton GM, Medzhitov R. Retroviral delivery of small interfering RNA into primary cells. Proc Natl Acad Sci U S A 2002;99:14943–14945. [PubMed: 12417750]

34. Meder D, Shevchenko A, Simons K, Fullekrug J. Gp135/podocalyxin and NHERF-2 participate in the formation of a preapical domain during polarization of MDCK cells. J Cell Biol 2005;168:303–313. [PubMed: 15642748]

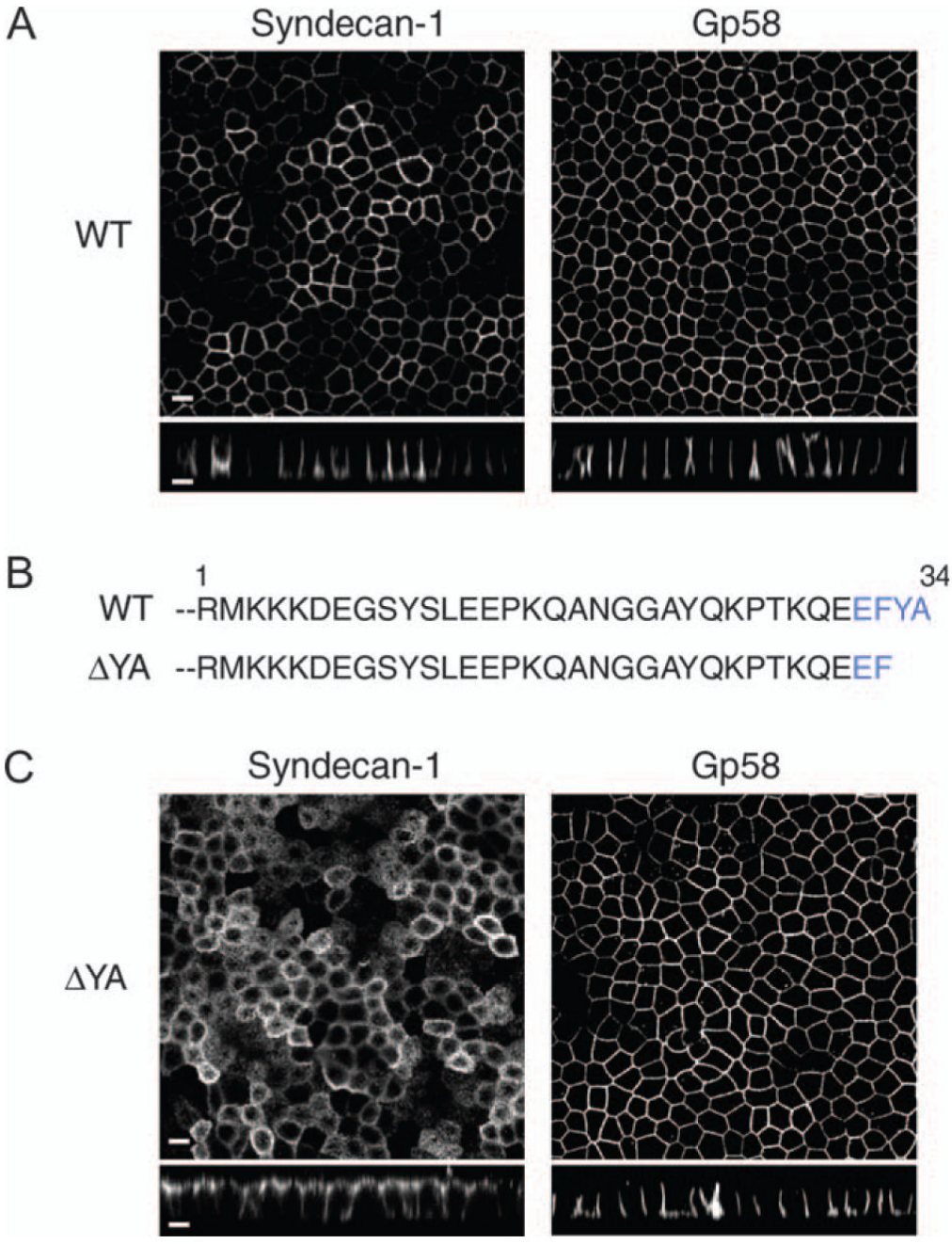

Figure 1. Truncation of the PDZ-binding motif causes apical mislocalization of syndecan-1

A) Polarized MDCK cells stably expressing WT syndecan-1 were fixed, permeabilized, processed for IF for syndecan-1 and gp58, and viewed by confocal microscopy. En face images and X–Z sections are shown. Bars, 10 μm. B) Sequence of the cytoplasmic tail of syndecan-1, with the PDZ-binding motif (blue). The last two residues were deleted in ΔYA. C) Polarized MDCK cells stably expressing ΔYA syndecan-1 were processed as in A. Bars, 10 μm.

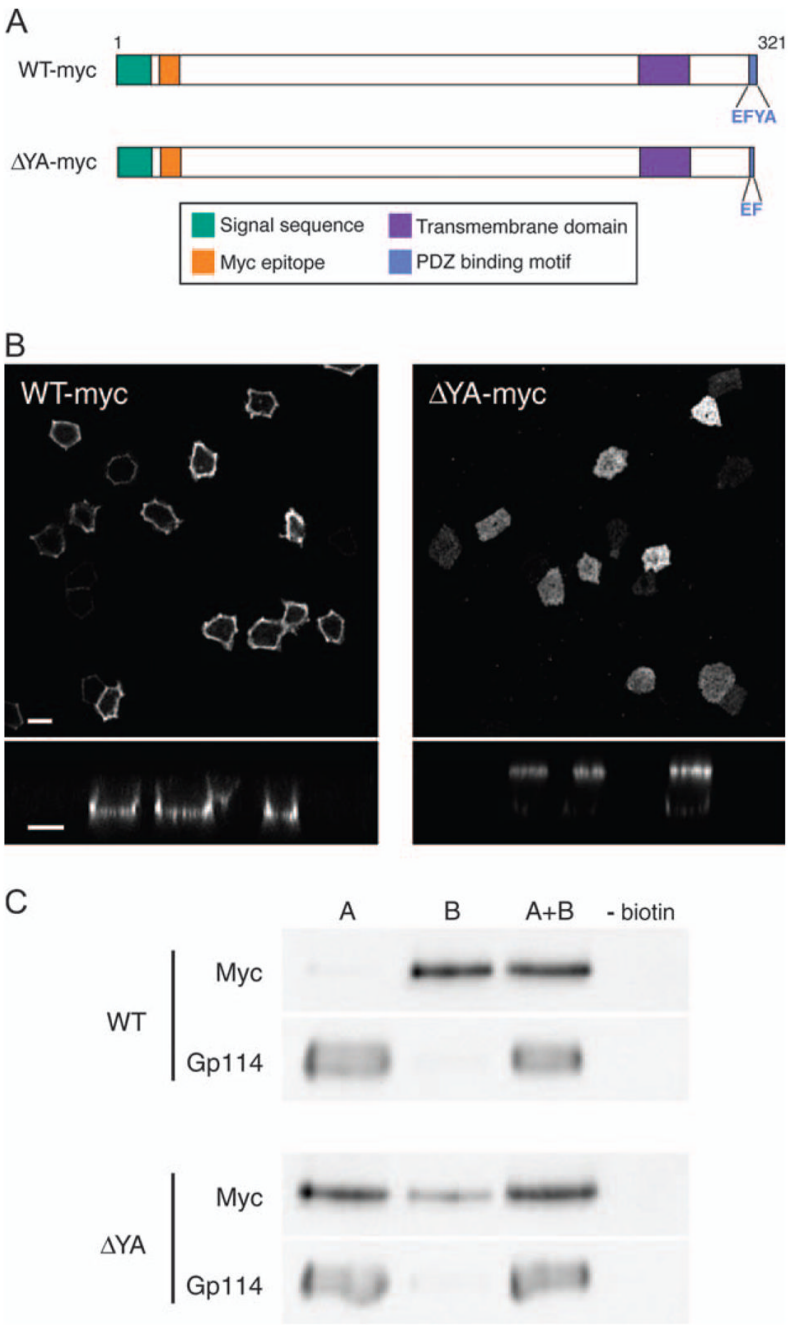

Figure 2. Biochemical characterization of ΔYA myc-syndecan-1 mislocalization

A) An myc tag was introduced at the N-terminus, after amino acid 22, five residues after the predicted 17-amino acid signal sequence. B and C) Polarized MDCK cells were infected with adenoviruses encoding either WT or ΔYA myc-syndecan-1 for 20 h. B) Cells were surface labeled for syndecan-1, processed for IF and analyzed by confocal microscopy. Bars, 10 μm. C) Cells were placed on ice and biotin was added to the apical domain (A), the basolateral domain (B) or both the apical and basolateral domains (A+B). Biotin was not added in one sample as a control. Biotinylated domain-specific surface protein was retrieved and processed for immunoblot.

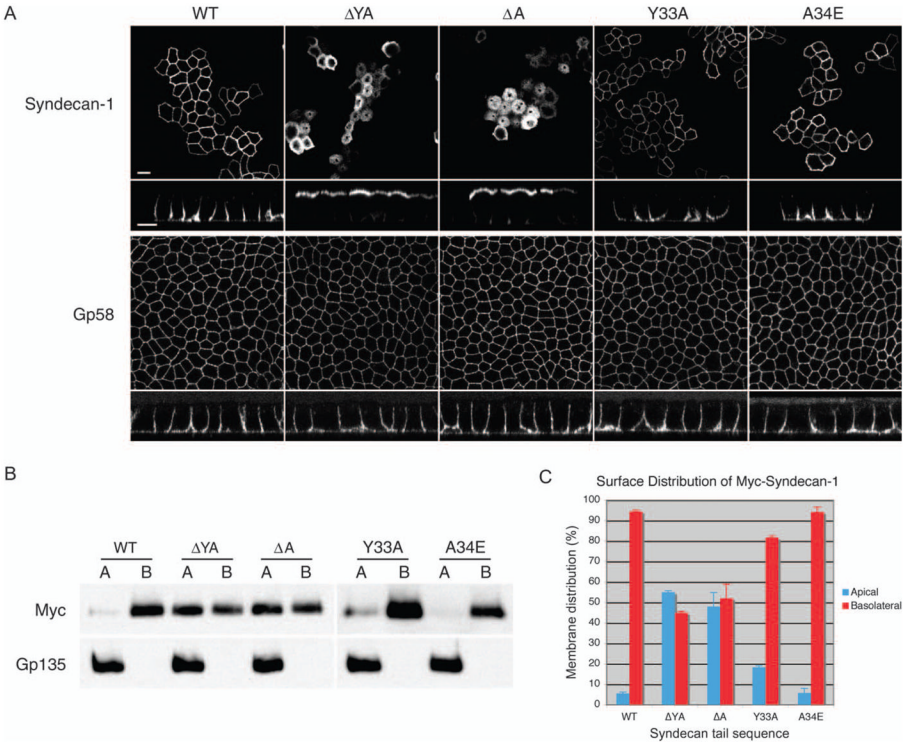

Figure 3. Additional mutations within the PDZ-binding motif cause apical mislocalization

A) Polarized MDCK cells stably expressing the indicated syndecan-1 mutant were surface labeled for syndecan-1, processed for IF and analyzed by confocal microscopy. Bars, 10 μm. B) Polarized MDCK cells stably expressing the indicated syndecan-1 mutant were placed on ice and biotin was added to the apical (A) or basolateral (B) domain. Samples were processed as in Figure 2C and quantified in C. Data represent mean values from two independent experiments and error bars indicate standard deviation.

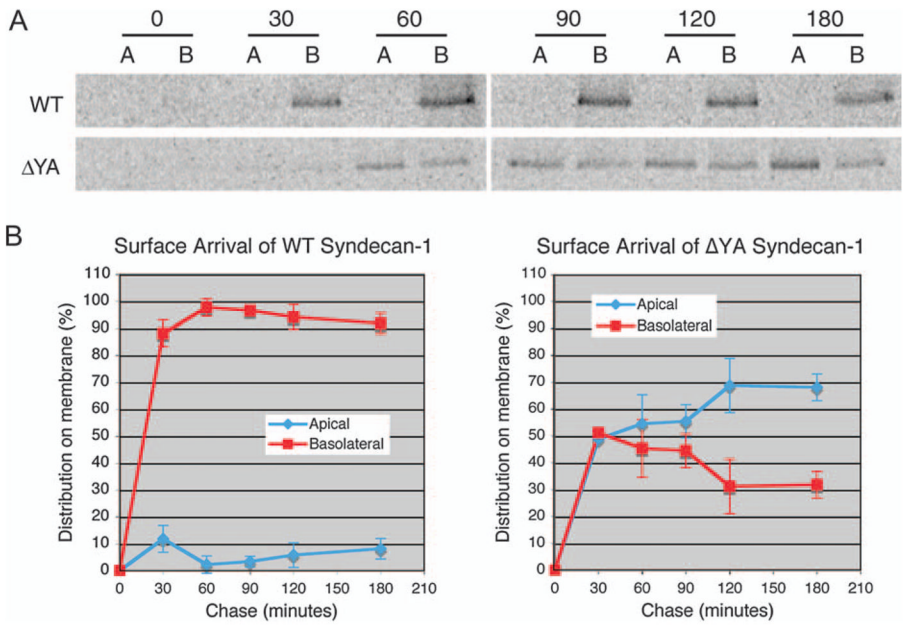

Figure 4. PDZ-binding motif targets syndecan-1 directly to the basolateral membrane

A) Polarized MDCK cells were infected with adenoviruses encoding WT or ΔYA myc-syndecan-1 for 20 h. Cells were pulsed for 15 min at 37°C with 2 mCi/ml ^{35}S-methionine and ^{35}S-cysteine, and chased for 0–3 h. At each time point, cells were placed on ice and biotinylated on the apical (A) or basolateral (B) domain. Total syndecan-1 protein was immunopre-cipitated and eluted. Biotinylated domain-specific surface syndecan-1 protein was retrieved and processed for SDS–PAGE and autoradiography. B) Quantification of A. Data represent mean values from two independent experiments and error bars indicate standard deviation.

Table 1

Syndecan-1 localization is unaffected by single or double knockdowns of syntenin, synectin, CASK or synbindin

Target	% Knockdown	Localization of syndecan-1
Single knockdowns		
Syntenin	91	Basolateral
Synectin	88	Basolateral
CASK	75	Basolateral
Synbindin	ND	Basolateral
Double knockdowns		
Syntenin	87	Basolateral
Synectin	79	
Syntenin	78	Basolateral
CASK	77	
Synectin	83	Basolateral
CASK	71	

ND, not determined.